Biofilm model development and process analysis of anaerobic bio-digestion of azo dyes

Mohammad Shaiful Alam Amin [a,b], Md. Salatul Islam Mozumder [b],
Frank Stüber [a], Jaume Giralt [a], Agustí Fortuny [c], Azael Fabregat [a], Josep Font [a,*]

[a] Universitat Rovira i Virgili, Departament d'Enginyeria Química, Avinguda Països Catalans, 43007 Tarragona, Catalunya, Spain
[b] Shahjalal University of Science and Technology, Department of Chemical Engineering and Polymer Science, Sylhet 3114, Bangladesh
[c] Universitat Politècnica de Catalunya, Departament d'Enginyeria Química, EUPVG, Av. Víctor Balaguer, s/n, 08800 Vilanova i la Geltrú, Catalunya, Spain

ARTICLE INFO

ABSTRACT

Ceramic-supported graphene oxide membrane bioreactors have already shown their potential for the anaerobic decolorization of wastewater containing azo dyes. The primary goal of this investigation was to develop a mathematical model that would be able to describe the steady-state behavior of this biodegradation process. The developed model was calibrated and validated using independent experimental data sets with various dye structure, feed concentration, hydraulic retention time (HRT), and support materials on which the biofilm was grown. The calibrated and validated model was used to analyze the intrinsic mechanism of the process and the main finding was that hydrolysis is the rate limiting step. Hydrolysis rate constant is decreased with increasing the complexity of the dye structure. Support materials with high electron transfer capacity increased the biofilm activity, therefore, increased the hydrolysis rate constant. Acetate concentration, used as an external carbon source, improved the dye removal efficiency. However, acetate to dye ratio did not have a direct relation to dye removal efficiency. Higher hydraulic retention time (HRT) increased the contact time between dye molecules and biofilm and enhanced the dye removal efficiency, too. However, it is essential to impose the right balance between HRT and external carbon sources to make the process feasible.

1. Introduction

The textile and garment sector still play a significant role in the growth of the global economy. In the rapid expansion of these industries, several issues have arisen related to huge water pollution. The main cause of this pollution is the extensive use and discharge of dyestuff, especially azo dyes, which represent 70% of the organic colorant chemicals (Berradi et al., 2019). A recent research found that about 744 tons of wastewater are generated while manufacturing one ton of dye (Li et al., 2015). Another statistics reported that nearly 200 000 tons of dyes are lost annually in the effluent streams during the dyeing and printing process, which are discharged into the aquatic systems (Yilmaz Ozmen et al., 2007). This enormous amount of dye-containing waste released into the environment consistently pollutes the lakes,

Abbreviations

b_h	Decay rate constant of anaerobic bacteria, h^{-1}
D_{NH}	Ammonium diffusion coefficient in water, $cm^2\ h^{-1}$
D_{O2}	Oxygen diffusion coefficient in water, $cm^2\ h^{-1}$
D_S	S_A, S_F, S_S diffusion coefficient in water, $cm^2\ h^{-1}$
D_H	S_H diffusion coefficient in water, $cm^2\ h^{-1}$
D_{SO2}	SO_2 diffusion coefficient in water, $cm^2\ h^{-1}$
f_I	Fraction of inert COD generated by biomass lysis
i_{NXB}	Nitrogen content in bacteria, mgN/mgCOD
i_{NXI}	Nitrogen content in inert particulate, mgN/mgCOD
k_h	Hydrolysis rate constant
K_{fe}	Saturation coefficient for fermentation of S_F, mgCOD/mL
K_A^H	Saturation coefficient for anaerobic digestion of S_A, mgCOD/mL
K_{NH}^H	Saturation coefficient for ammonium–nitrogen on anaerobic digestion, mgO_2/mL
n	Power index for hydrolysis
q_{fe}	Maximum rate for fermentation, h^{-1}
S_A	Fermented product concentration, mgCOD/mL
S_F	Hydrolyzed organic substrate concentration, mgCOD/mL
S_H	Digested product concentration, mgCOD/mL
S_S	Dye concentration, mgCOD/mL
S_{NH}	Ammonium concentration, mgCOD/mL
S_{SO2}	Sulfur concentration, mgCOD/mL
V_{NH}	Fraction of nitrogen in dye
V_S	Fraction of sulfur in dye
X_I	Inert particulate concentration, mgCOD/mL
X_H	Anaerobic bacteria concentration, mgCOD/mL
Y_H	Anaerobic Yield coefficient
μ_{max}^{AD}	Maximum specific growth rate of anaerobic bacteria, h^{-1}

rivers, and other water reservoirs (Benkhaya et al., 2020; Jankowska et al., 2021). Therefore, it is essential to treat these textile effluents before discharge to save and maintain healthy aquatic life.

Numerous approaches, including physical, chemical, physicochemical, and biological processes, have been examined independently or combined to treat the dye-containing wastewater. In contrast to biological process, physical and chemical processes are more expensive, resulted in the production of more sludge, and required further treatment (Iqbal et al., 2022). Advanced oxidation processes, including Photo-Fenton and photocatalytic degradation, are established technologies for treating dye-containing wastewater (Hammad et al., 2021; Han et al., 2018; Uddin et al., 2012). Nonetheless, it is still incompatible with industrial use due to a large-scale operation's reasonable expense and incompetence. As a result, biotreatment of azo dye wastewater is still a viable option because of its low costs and minimal environmental impact (Takkar et al., 2022). Biodecolorization of dyestuff molecules can be accomplished using anaerobic or aerobic bacteria (mixed or pure), activated sludge, and membrane bioreactor (Bibi et al., 2020; Nguyen et al., 2020; Vu et al., 2020). However, considering the efficiency, generation of secondary sludge and toxic byproduct, installation, and operating cost; the integration of membrane filtration and anaerobic biodegradation of textile dyes has proven to be very attractive (Amin et al., 2021, 2022a,b). Recently, we demonstrated that the Ceramic-supported Carbonized Membrane (CSCM), which was synthesized by the carbonization of Matrimid 5218 polyimide solution, had the ability to complete the decolorization of azo dyes (Amin et al., 2021). During the anaerobic biodegradation of azo dye, the nanosized CSCM helps to generate an active biofilm by retaining the microorganism on its surface. In addition, this layer enhanced the electron transfer mechanism between the azo bond and microorganisms to increase the biodegradation rate (Mezohegyi et al., 2007). Like other Besides, this membrane improves the treatment performance through the retention of the dye molecules and biodegradable products. Amin et al. (2022a) also investigated the influence of the conductive Ceramic-supported Graphene Oxide Membrane (CSGOM) derived from the exfoliated graphene oxide (GO) solution on biodecolorization performance, and the results showed that compared to CSCM, CSGOM is even more effective for the anaerobic color removal of azo dye under identical operating conditions. The color removal efficiency was directly influenced by several factors such as selective activity of microbial entities in the aqueous medium, supplementary carbon sources, dye structure, concentration, and retention time. The mixed microbial consortia involved in anaerobic decolorization of dye molecules

convert the soluble substrate into volatile acids or alcohols that serve as a competitive substrate for methanogenic, sulfate-reducing, and acetogenic bacteria (Georgiou et al., 2004; Yoo et al., 2001). The experimental evaluation of these parameters within a compact membrane bioreactor is very difficult and time-consuming.

Thus, mathematical modeling is essential for addressing issues associated with this novel process. The computer-aided model facilitates the precise understanding or description of the biodegradation of azo dyes and boosts the decolorization efficiency. Moreover, the complex biological process simulation predicts the influencing parameters and kinetics that lead to the process limiting steps and recommends relevant experiments. It is generally agreed that the Activated Sludge Model (ASM) represents the current state of the art for the biological wastewater treatment processes. The removal of organic carbon and nitrogen, in addition to biological phosphorus, has resulted in the development of a number of variations of the ASM model (Petersen et al., 2002) but there were no evaluation on the effect of supporting materials to the microbial activities. However, the unmodified ASM models described by Henze et al. (2000) has been applied successfully over membrane bioreactors (Fenu et al., 2010). The ASM approach for treating municipal and industrial wastewater has been studied extensively afterward, both with and without modifications (Orhon et al., 2021a,b; Petersen et al., 2002). In case of anaerobic biodegradation of dyes, very few mathematical models have been constructed, mainly focused on the optimization of process variables using response surface methodology (Sonwani et al., 2020). However, to the best of our knowledge, no model is available to analyze the interaction between biofilm and support materials, which is also act as a membrane.

With the aforesaid limitations in dye biodegradation research, this work attempts to understand the mechanism of biodecolorization of azo dye under an integrated anaerobic membrane bioreactor scheme. Therefore, the present study has modified the Activated Sludge Model-2 (ASM2) model to be applied for a membrane supported biofilm process. The modified model was first calibrated and validated with independent experimental datasets and then used it scenario analysis. Thus, this model was applied to assess all the operating and process variables parameters, such as dye structures, initial dye concentration, permeate flux, and hydraulic retention time (HRT), that need to be controlled in real cases. Hydrolysis behavior of complex dye molecules and effect of support materials for biofilm aiming to biodegradation of dyes were assessed. To the best of our knowledge, the interaction among the HRT, external carbon source and dye concentration in a CSGOM support biofilm reactor for dye removal has been assessed for the first time. The steady-state model behavior was considered in all cases to evaluate the overall process performance.

2. Materials and methods

2.1. Preparation of bioreactors

The biofilm in a single bioreactor using either ceramic-supported carbon membrane (CSCM) or ceramic-supported graphene oxide membrane (CSGOM) support materials were developed for the bio-digestion of dyes. In order to build the CSCM, a membrane precursor containing 10% wt. Matrimid solution was carbonized over the ceramic support. On the other hand, CSGOM was created using a standard technique outlined elsewhere (Giménez-Pérez et al., 2016). In this case, 1 mg/mL graphene oxide solution was used to make the CSGOM support material. The biofilm was produced seeding secondary anaerobic sludge collected from a municipal WWTP (Reus, Spain), which was placed over the CSCM and CSGOM support materials and left to grow.

2.2. Process configuration

A controllable vacuum filtration unit (TAMI Industries, Nyons, France), in which CSCM and CSGOM were installed as filters and support for biofilm growth, was used. Three different types of dyes, monoazo AO7 (ACROS Organics, ref. 416561000), diazo RB5 (Sigma Aldrich, ref. 306452), and triazo DB71 (Sigma Aldrich, ref. 212407), were selected to generate the artificial wastewater that was mixed with sodium acetate (Sigma Aldrich, ref. 110191) maintaining the absolute concentration (in mg/mL) ratio 1:3. The dye and sodium acetate (SAc) mixture was then mixed with 1 mL of each basal medium (BM) to make the feed solution. There were six basal mixtures; the elements contained, and composition are listed in Table 1.

All the chemicals (Sigma Aldrich, Spain) used in this study were analytical grade, and the solutions were made with Milli-Q water (Millipore Milli-Q system, Molsheim, France). The feed solution was kept at 1 °C to prevent microbial growth in the feed solution tank. Nitrogen gas (>99.99%, Linde) was sparged through the feed tank to maintain it under anaerobic conditions (negative redox potential) and, also, for controlling the permeate flux by setting the needed pumping pressure. The compact bioreactor was run under dead-end filtration mode at a temperature of 37 ± 1 °C. Samples were collected at regular intervals, and then the dye concentration, acetate concentration, ammonium concentration, and COD were immediately analyzed.

2.3. Analytical procedure

The decolorization was measured in a visible/UV spectrophotometer (DINKO Instruments, Barcelona, Spain), whereas the maximum absorption wavelength was set at 484 nm for AO7, 597 nm for RB5, and 585 nm for DB71. Acetate

Table 1
Composition and concentration of the different basal media.

Basal medium (BM)	Minerals	Concentration (mg/L)
BM 1	$MnSO_4 \cdot H_2O$	0.15
	$CuSO_4 \cdot 5H_2O$	0.28
	$ZnSO_4 \cdot 7H_2O$	0.46
	$CoCl_2 \cdot 6H_2O$	0.26
	$(NH_4)_6Mo_7O_{24}$	0.28
BM 2	K_2HPO_4	21.75
	$Na_2HPO_4 \cdot 2H_2O$	33.40
	KH_2PO_4	8.50
BM 3	$FeCl_3 \cdot 6H_2O$	29.06
BM 4	$CaCl_2$	13.48
BM 5	$MgSO_4 \cdot 7H_2O$	15.20
BM 6	NH_4Cl	190.90

Table 2
Stoichiometric matrix A_{ij}.

A_{ij}	i component →	S_S [mgCOD/mL]	S_F [mgCOD/mL]	S_A [mgCOD/mL]	S_H [mgCOD/mL]	S_{NH} [mgN/mL]	S_{SO2} [mgS/mL]	X_H [mgCOD/mL]	X_I [mgCOD/mL]
j process ↓									
1. Anaerobic hydrolysis		−1	1- $(V_{NH}+V_S)$			V_{NH}	V_S		
2. Anaerobic fermentation			−1	1					
3. Anaerobic digestion				−1/Y_H	(1- Y_H)/Y_H	-i_{NXB}		1	
4. Decay of X_H			1-f_I			i_{NXB} - f_I i_{NXI}		−1	f_I

Table 3
Kinetic rate expressions.

j process	Kinetic rate expression	Equation
1. Anaerobic hydrolysis	$\rho_H = k_h \cdot S_{S(in)}^{-n} S_S \cdot X_H$	(1)
2. Anaerobic fermentation	$\rho_F = q_{fa} \cdot \dfrac{S_F}{K_{fe} + S_F} \cdot X_H$	(2)
3. Anaerobic digestion	$\rho_{AD} = \mu_{max}^{AD} \cdot \dfrac{S_A}{K_A^H + S_A} \cdot \dfrac{S_{NH}}{K_{NH}^H + S_{NH}} \cdot X_H$	(3)
4. Decay of X_H	$\rho_D = b_H \cdot X_H$	(4)

concentration in both feed and permeate solution was determined by high-performance liquid chromatography (HPLC) on a C18 Hypersil ODS column applying a gradient of methanol–water mobile phase with a flow rate of 1 mL/min (García-Martínez et al., 2015). Portable chemical oxygen demand (COD) test kit (Lovibond Vario 2 420 721 and 2 420 722) was used to measure the COD influent dye containing wastewater and permeate. The ammonium-N was determined by the salicylate method (Lovibond method 66) using the Lovibond testing kit (Vario 535 650).

2.4. Model development

The anaerobic digestion model was developed based on Activated Sludge Model-2 (ASM2) to examine the anaerobic bio-digestion of dye using a single bed biofilm reactor. An empirical hydrolysis rate equation was developed from the experimental datasets.

The model for anaerobic dye decomposition takes into account four main processes: (1) anaerobic hydrolysis of dye (S_S); (2) fermentation of fermentable materials (S_F); (3) anaerobic digestion of fermented product (S_A), and (4) biomass decay. The model stoichiometry and kinetics are listed in Tables 2 and 3, respectively. The stoichiometric and kinetic parameter values are listed in Table 4.

It is assumed that all dyes undergo hydrolysis first and then anaerobic fermentation and subsequent digestion. The first process, hydrolysis of dye (S_S), followed simple reaction kinetics, proportional to dye concentration and presence of microorganisms. As a result, the fermentable materials (S_F) were produced through the hydrolysis of complex dye molecules. Fermentable materials are then converted to fermented products (S_A) by following anaerobic fermentation or organic decomposition (second process) that followed Monod kinetics as described in ASM2 (Henze et al., 2000).

It must be noted that, in this study, acetate was considered as the fermented product (S_A). The S_A was then transformed through anaerobic digestion (third process) and converted to carbon dioxide and methane (S_H). Anaerobic digestion depends on the S_A and ammonium concentration. The growth of microorganisms resulted from the anaerobic digestion, where ammonium nitrogen played a significant role. According to ASM2, it was also considered that hydrolysis and fermentation did not take part in microbial growth. The microorganisms (X_H) produced by the digestion process took

Table 4

Stoichiometric and kinetics parameters.

Parameter	Value	Units	Reference
Y_H	0.06	mgCOD/mgCOD	Sun et al. (2016)
μ_{max}^{AD}	20.0325	h^{-1}	Estimated
k_h	Biofilm on CSGOM: AO7: 41.51 ± 2.56 RB5: 4.87 ± 0.31 DB71: 6.46 ± 0.57 Biofilm on CSCM: DB71: 0.841 ± 0.053	$(mgCOD)^{n-1}/$ $(L^{n-1}.h)$	Estimated
n	1.715 ± 0.108		Estimated
K_A^H	0.0760	mgCOD/mL	Sun et al. (2016)
K_{NH}^H	0.0300	mgN/mL	Sun et al. (2016)
b_H	0.00083	h^{-1}	Sun et al. (2016)
q_{fe}	20.033	h^{-1}	Assumed same as μ_{max}^{AD}
K_{fe}	0.0040	mgCOD/mL	Henze et al. (2000)
i_{NXB}	0.0700	mgN/mgCOD	Henze et al. (2000)
i_{NXI}	0.0700	mgN/mgCOD	Assumed same as i_{NXB}
f_I	0.0800	mgCOD/mgCOD	Henze et al. (2000)
V_{NH}	AO7: 0.0422 RB5: 0.062 DB71: 0.0570	mgN/mgCOD	From stoichiometric calculation
V_S	AO7: 0.0481 RB5: 0.1700 DB71: 0.074	mgS/mgCOD	From stoichiometric calculation
D_{NH}	0.0625	$cm^2\ h^{-1}$	Williamson and McCarty (1976)
D_{O2}	0.0917	$cm^2\ h^{-1}$	Picioreanu et al. (1997)
D_S	0.0417	$cm^2\ h^{-1}$	Hao and van Loosdrecht (2004)
D_H	0.0538	$cm^2\ h^{-1}$	Stewart Philip (2003)
D_{SO2}	0.0917	$cm^2\ h^{-1}$	$\approx D_{O2}$ (Assumed)

(1) After unit conversion, using a typical biomass composition of $CH_{1.8}O_{0.5}N_{0.2}$, corresponding with 1.3659 mgCOD/mg (Volcke et al., 2010)

(2) ThOD (mgCOD/mg): $S_A = 0.78$, AO7 = 1.987, RB5 = 1.331, DB71 = 1.790

(3) Conversion of ASM2 and ASM2d-values given by Henze et al. (2000) at 10 °C and 20 °C to 37 °C using temperature relationship proposed by these authors (in ASM3):

$$\theta_T = \frac{\ln(k(T_1)/k(T_2))}{T_1 - T_2}.$$

part in all biological activities. The amine group and sulfur present in dye molecules were converted to ammonium and hydrogen sulfite through anaerobic hydrolysis.

Therefore, the process was stated as completely anaerobic, so oxygen was not considered as an operating variable in this study. Carbon dioxide and methane produced during digestion did not affect the process and hence were not accounted in the global kinetics.

The biomass decay followed the death-regeneration concept in which the living cells were directly converted to the soluble organic substrate and a fraction of inert materials (Van Loosdrecht and Henze, 1999). Decay was first-order kinetics, and its rate-limited steps over the hydrolysis of decay product. Therefore, hydrolysis merged with the decay, and fermentable materials were directly produced from the decay of biomass (Mozumder et al., 2014).

2.5. Configuration, simulation parameters and initial conditions

An one-dimensional biofilm model, only considering gradients through biofilm depth was set up to describe the process. The model was implemented in the Aquasim software (Reichert, 1994). The reactor had a fixed volume of 5 mL; same as that experimentally used. A layer of biomass was assumed to grow on the support materials (CSCM or CSGOM) with a surface area of 13.1 cm^2 for a predefined biofilm thickness of 2 μm. The biofilm was generally dense and rigid, and biofilm porosity was assumed to be constant (25%). The density of the biomass and inert materials were considered as 60 mg VSS/mL (van Benthum et al., 1995) and, according to Henze et al. (2000), it corresponds to 80 mg COD/mL (Henze et al., 2000).

The process was evaluated in both experimental and model simulation for an influent feed solution containing dye and acetate, maintaining the dye concentration three times less than acetate (1:3 molar ratio), even when dye flow rate varied from 0.066 to 0.131 mL/h. The dye concentration ranged from 0.05 mg/mL to 0.10 mg/mL. It was assumed that there was

Table 5
Experimental removal of AO7 by CSGOM-biofilm reactor at various hydraulic retention times and dye feed concentration.

HRT (h)	AO7 concentration in feed ($S_{S(in)}$) (mgCOD/mL)	% Dye removal
0.040	0.099	98.3
	0.149	97.8
	0.198	97.4
0.027	0.099	97.5
	0.149	96.8
	0.198	95.9
0.020	0.099	96.8
	0.149	95.9
	0.198	94.8

initially no other fermentable organic matter (S_F) in the inflow. The initial concentrations of dye and substrate in the bulk liquid were assumed equal to influent concentrations. The processes were operated at 37 °C. Steady-state simulations were performed to evaluate the process. The interactive effect of dye concentration, HRT, and influent fermented product (S_A) were investigated by following COD through steady-state calculations for different combinations of their concentrations and variation of feed flow rate.

2.6. Model calibration and validation

The model calibration was conducted to determine model parameters represented by constant variables from available data. The parameters were estimated using AQUASIM by minimizing the sum of the squares of the weighted deviations between measurements and simulation outcomes following Eq. (5).

$$\chi^2(P) = \sum_{i=1}^{m} \left(\frac{y_{\exp,i} - y_{i(P)}}{\sigma_{\exp,i}} \times 100 \right)^2 \tag{5}$$

where, $y_{exp,i}$ is the experimental value, $\sigma_{exp,i}$ is its standard deviation, $y_{i(p)}$ is the estimation of the corresponding model parameter P, and m is the number of data points.

The model validation was conducted through the visual comparison of experimental values and steady-state simulation outcomes. Moreover, the validation was confirmed by calculation of deviation (%) defined by Eq. (6). Less than 10% deviation was considered as an acceptable value.

$$\% \text{ deviation} = \left(\frac{y_{\exp,i} - y_{i(P)}}{y_{\exp,i}} \times 100 \right) \tag{6}$$

3. Results and discussion

The model behavior was evaluated for three different dyes; monoazo AO7, diazo RB5 and triazo DB71. Model calibration and validation were performed based on independent experimental data sets. The model calibration was based on biodegradation of monoazo AO7 with three different concentration and three different HRT, while biodegradation of diazo RB5 and triazo DB71 with three different concentration and HRT were accounted for during validation. Different scenarios were analyzed to find out the optimal balance between external organic carbon and HRT in view of maximal dye removal.

3.1. Model calibration

To describe the anaerobic biodegradation of dye, the developed model was calibrated on independent experimental datasets. For the model calibration, continuous mode biodegradation was selected using monoazo AO7 dye with different feed concentrations and flow rates. In this case, the biofilm was developed on ceramic-supported graphene oxide membrane (CSGOM). In all the cases, acetate was set three times higher than dye concentration (in mg/mL), although it was fully consumed through the biodegradation process. The results showed that steady-state AO7 concentration in permeate was higher with increasing feed concentration and decreasing HRT. It must be noted that this HRT, as defined, differs from those usually applied in conventional computation. Instead of using the total volume of the bioreactors (5 mL), only the estimated biofilm volume (0.00262 mL) was considered for subsequent calculation, as the biodegradation of azo dyes is assumed to happen essentially in the biofilm, while it is neglected in the rest of reactor volume. Therefore, this biofilm volume was used to calculate the estimated actual hydraulic retention time for this anaerobic biodecolorization process. Maintaining 0.04 h of HRT, the permeate AO7 concentration was increased from 0.00166 ± 0.00052 mgCOD/mL to 0.00520 ± 0.00096 mgCOD/mL with increasing feed concentration from 0.099 mgCOD/mL (0.05 mg/mL) to 0.198 mgCOD/mL (0.10 mg/mL). Accordingly, the removal decreased from 98.3% to 97.4% (Table 5).
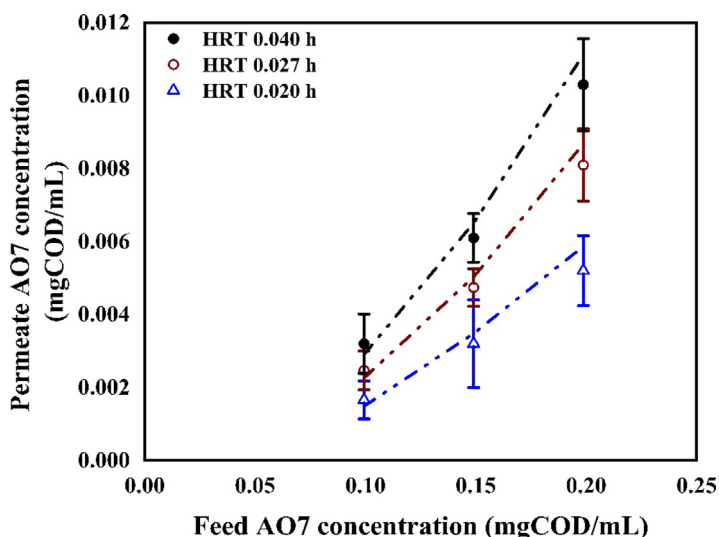
Fig. 1. Comparison between experimental and predicted outcomes of AO7 removal at steady-state using a CSGOM-biofilm reactor (points are the experimental values and lines are predictions from the model).

A higher feed flow rate reduces the HRT, which adversely affects the dye removal efficiency. Thus, the HRT decrease, from 0.04 h to 0.02 h, dropped the dye removal efficiency from 97.4% to 94.8% (Table 5). The hydrolysis rate constant (k_h) for AO7 biodegradation, the power index of inflow dye concentration in feeding solution (n) and maximum specific growth rate of the anaerobic organism (μ_{max}^{AD}) were determined from the model calibration. The experimental datasets with fixed HRT, 0.04 h, at various inflow dye concentrations, from 0.099 mgCOD/mL to 0.198 mgCOD/mL, were used for the calibration. The estimated value of the hydrolysis constant, k_h, was found to be 41.5 $\pm$ 2.6 (mgCOD)$^{n-1}$/(L^{n-1}.h), while n was 1.71 $\pm$ 0.11, and μ_{max}^{AD} was 20.0 h^{-1} for all the feed concentrations.

3.2. Model validation

The calibrated model was validated for several HRT in the CSGOM-biofilm reactor and the different AO7 dye feed concentrations. Using the estimated hydrolysis rate constant, the power index (n), and maximum specific growth rate of the anaerobic organism (μ_{max}^{AD}), the model could describe the steady-state behavior of the biodegradation of AO7 very well with deviations below 10% (Fig. 1 and Table A.1).

The high hydrolysis constant in this study was due to the reduced detachment of biofilm with the support material GO and high electron transfer rate (Amin et al., 2022a) that improve the effective microbial activities (García-Martínez et al., 2015) as well as ensure biodegradation of dye with a high efficiency. Additionally, the high adaptability of the specific dye-consuming bacteria presents in the anaerobic biofilm enhanced the decolorization of azo dyes, thus giving high hydrolysis constant. Comparison between the experimental and model output is summarized in Table A.1.

3.2.1. Model evaluation with various types of dye

Anaerobic biodegradation in a CSGOM-biofilm reactor was also evaluated for three different types of dye; monoazo AO7, diazo RB5 and triazo DB71. In both cases, the dye concentration was changed from 0.05 mg/mL ($\approx$0.066 mgCOD/mL RB5 and 0.089 mgCOD/mL DB71) to 0.10 mg/mL ($\approx$0.133 mgCOD/mL RB5 and 0.179 mgCOD/mL DB71) whilst feed flow rate was varied from 0.066 mL/h to 0.131 mL/h to set the hydraulic retention time from 0.040 h to 0.020 h.

Hydraulic retention time (HRT), which must be understood as contact time, has a critical relation with color removal rate. Due to the extended HRT, the system may efficiently treat dye-containing wastewater, even at a higher initial feed concentration (da Silva et al., 2012; Oh et al., 2004). In this CSGOM bioreactor, we also observed a similar pattern, wherein increasing hydraulic retention time improved the dye removal efficiency and, consequently, decreased the dye concentration in permeate (Table 6). Moreover, initial dye concentration and dye structure significantly affect the anaerobic decolorization kinetics. Dyestuff with a simple structure and low molecular weight showed a higher biodegradation rate than complex and high molecular weight dyes (da Silva et al., 2012; Solís et al., 2012). As comparing the three types of dyes; AO7 showed better removal efficiency, and DB71 showed the lowest (Tables 5 and 6), following the number of azo bonds in the respective molecule. It is noted that, under the same operating conditions, the COD of the effluents in the anaerobic bioreactor was tracked regularly and ensure that all dyes and their intermediate products were effectively removed.

However, it is not possible to apply the estimated hydrolysis constant (k_h), power index of inflow feed concentration (n), and maximum specific growth rate of the anaerobic organism (μ_{max}^{AD}) obtained from the biodegradation of AO7; because
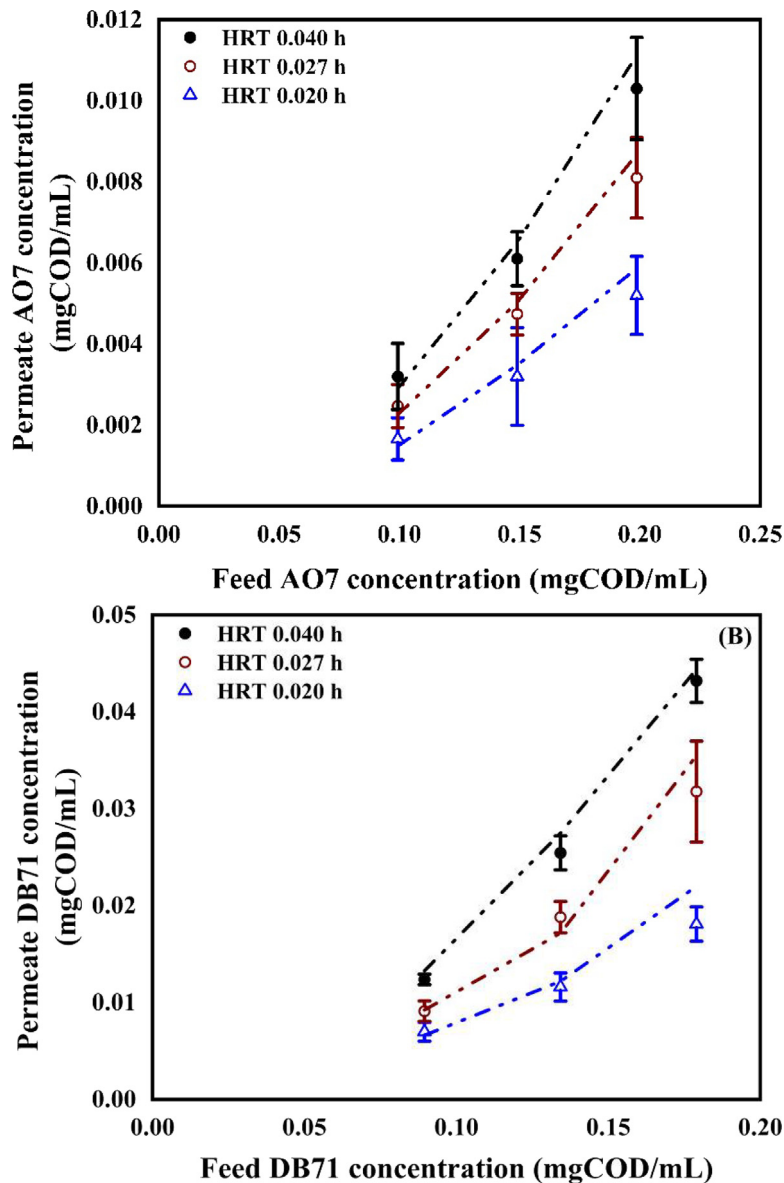
Fig. 2. Model validation for (A) RB5 and (B) DB71 removal in a CSGOM-biofilm reactor (points are the experimental values, and lines are simulation outcome).

it is not able to describe the steady-state behavior of RB5 and DB71 (data was not shown). As the dye structures and functionalities are not similar to each other; the hydrolysis rate constant can hardly be expected to be the same and needs to be re-estimate for these dyes. The estimated hydrolysis constants (k_h) were thus 4.87 ± 0.31 $(mgCOD)^{n-1}/(L^{n-1}.h)$ ($\chi^2 = 0.00009$) for RB5 and 6.64 ± 0.57 $(mgCOD)^{n-1}/(L^{n-1}.h)$ ($\chi^2 = 0.00007$) for DB71. Using these re-estimated k_h, the model predictions agreed well with the experimental values of dye concentration in permeate at steady-state (Fig. 2). The percentage deviation associated with HRT, dye feed concentration and dye types were below 10%, which demonstrates the goodness of the model fit (as seen in Tables A.2–A.3).

The hydrolysis rate constant was indeed quite different for each type of dye. Increasing molecular weight as well as complexity of dye structure lowers the hydrolysis capacity of the microorganisms, which results in lower hydrolysis constant (Table 7). Tombari et al. (2007) found that the change of configurational and vibrational partition functions has a significant effect on hydrolysis. Kura (1987) analyzed the hydrolysis for different membered inorganic cyclophosphates and found that the lowest membered cyclotriphosphate showed the most rapid hydrolysis (Kura, 1987). In addition, there was a wide variation of hydrolysis due to structural variation (Culbertson, 1951). Similarly, in this study, it has been found
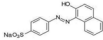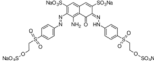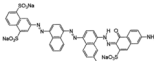
Table 6

RB5 and DB71 removal in a CSGOM-biofilm reactor for several hydraulic retention times and dye concentrations.

HRT (h)	Reactive Black 5		Direct Blue 71	
	Feed concentration $(S_{S(in)})$ (mgCOD/mL)	% Dye removal	Feed concentration $(S_{S(in)})$ (mgCOD/mL)	% Dye removal
0.040	0.066	95.9	0.089	92.2
	0.099	94.5	0.134	91.4
	0.133	93.0	0.179	89.9
0.027	0.066	93.4	0.089	89.8
	0.099	90.6	0.134	86.0
	0.133	88.6	0.179	82.2
0.020	0.066	90.6	0.089	86.7
	0.099	88.1	0.134	81.5
	0.133	86.3	0.179	76.0

Table 7

Relation between the dye properties (Amin et al., 2021) and estimated hydrolysis constants for CSGOM-biofilm.

Dye information	Dye structure	Estimated hydrolysis constant, k_h $(mgCOD)^{n-1}/ (L^{n-1}.h)$
Acid Orange 7: $C_{16}H_{11}N_2NaO_4S$, MW = 350.32 g/moL		1.43 ± 0.06
Reactive Black: 5 $C_{26}H_{21}N_5Na_4O_{19}S_6$, MW = 991.8 g/moL		0.29 ± 0.01
Direct Blue 71: $C_{40}H_{23}N_7Na_4O_{13}S_4$, MW = 1029.9 g/moL		0.26 ± 0.02

that the hydrolysis rate constant decreased with a growing molecular weight that also correlates here with the higher number of azo bonds in the dye molecules (Table 7).

3.2.2. Model evaluation with different supports

DB71 removal data were employed to find out the effect of support material for the biofilm formation, i.e., CSCM and CSGOM. The removal efficiency was quite higher for the biofilm growing on CSGOM compared to CSCM (Fig. 3). Biofilm over CSGOM gives, at steady-state, a dye removal of 92.2% for 0.089 mgCOD/mL DB71 feed concentration and 0.040 h of HRT, but 22% less removal was shown for CSCM support. The removal efficiency was also lowered as dye concentration increases and HRT decreases. For 0.020 h HRT, 50% less removal was encountered for CSCM-biofilm compared to CSGOM-biofilm.

The developed model was calibrated against data shown in Fig. 3 and the estimated hydrolysis constant (k_h) for CSCM was calculated to be 0.84 ± 0.05 $(mgCOD)^{n-1}/(L^{n-1}.h)$ ($\chi^2 = 0.000098$), while it was much higher for CSGOM ($k_h = 6.46 \pm 0.57$ $(mgCOD)^{n-1}/(L^{n-1}.h)$). The low hydrolysis constant for CSCM supporting biofilm is attributed to the lower electron transfer capacity compared to CSGOM. It indicated that the support material with high electron transfer ability enhances the hydrolysis, which eventually increases the dye removal efficiency.

Anyway, the calibrated model was able to reproduce very well the DB71 removal using CSCM based biofilm reactor with a deviation below 10% (Fig. 4 and Table A.4).

3.3. Scenario analysis

The anaerobic bio-digestion of the azo dye was investigated using scenario analysis to identify the probable best circumstances or conditions for process optimization. The following sections detail the optimum conditions for the maximum biodecolorization by adjusting the external carbon source (acetate), acetate to dye ratio, and the HRT.

3.3.1. Effect of external carbon source on anaerobic bio-digestion of dyes

The simulation was conducted with various acetate to dye ratios by changing their concentrations in the feed solution. The flow rate as well as HRT was kept constant at 0.027 h. The effect of acetate concentration on dye removal was evaluated based on steady-state dye concentration in permeate that was translated as percentage removal as a function of acetate to dye ratio and shown in Fig. 5.
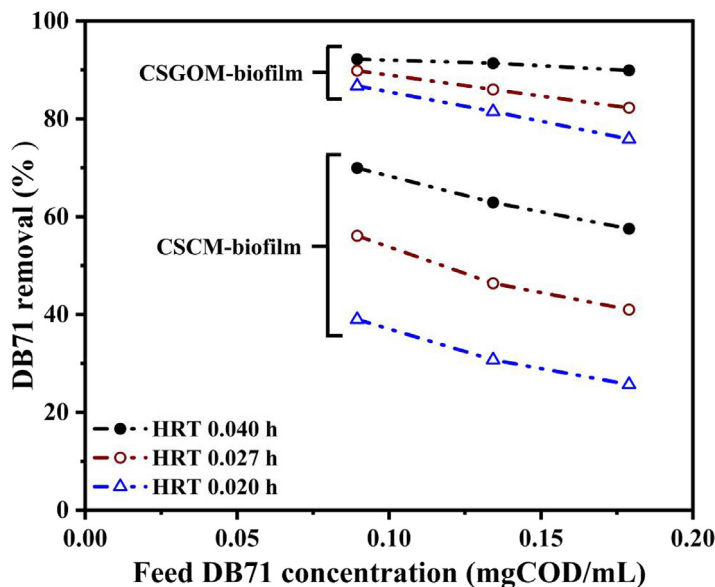
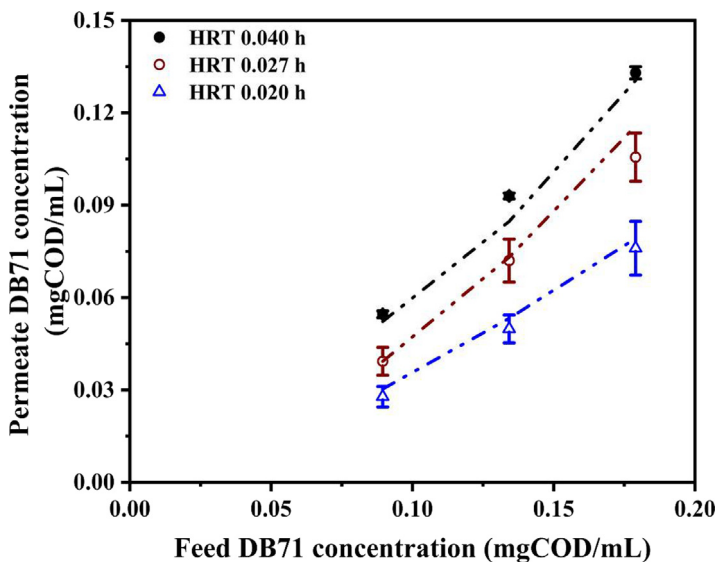**Fig. 3.** Comparison of DB71 removal efficiency of CSGOM-biofilm and CSCM-biofilm.

Fig. 4. Comparison between experimental and predicted behavior at steady-state for DB71 removal using biofilm on CSCM (points are the experimental values and lines are simulation outcome).

The results showed that the dye removal efficiency was increased as acetate (act as electron-donors) concentration increases in line with findings from other studies (Cui et al., 2016b; Pandey et al., 2007; Thung et al., 2017). At the same acetate to dye ratio, the removal efficiency was higher for low dye concentration. The dye removal efficiency was also decreased with the increasing molecular weight and complexity of dye. In absence of any external organic substrate (acetate), over 85% AO7 removal was still observed for 0.40 mgCOD/mL dye concentration (Fig. 5A) but for RB5 it was just 24% (Fig. 5B) while for DB71 it was 26% (Fig. 5C). Oppositely, more than 90% dye removal was found for both RB5 and DB71 by applying an acetate to dye ratio of 5. Easily fermentable organic materials like acetate give advantages to the microorganisms to grow and stimulate the hydrolysis process, thus the removal efficiency. The presence of acetate facilitated the easy transferability of electrons that promoted a faster degradation of azo dye, which suggests that a denser current of electrons helps the reductive break of the azo bond (Cui et al., 2016a). The increase of external carbon sources also promotes an easier development of biofilm and biomass formation and allows reaching a higher dye removal rate.
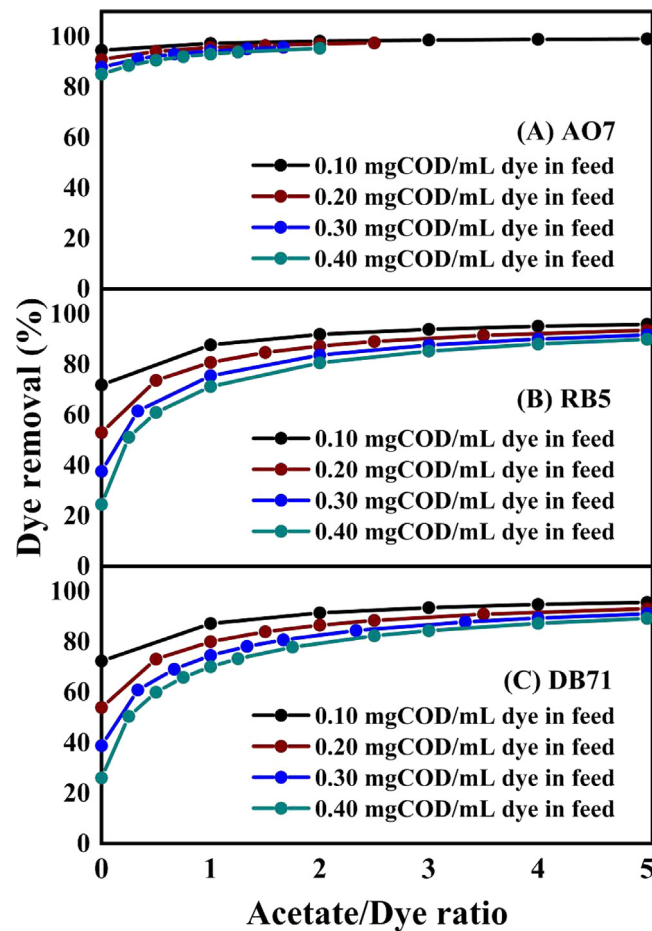
Fig. 5. Effect of acetate to dye ratio on (A) AO7, (B) RB5, and (C) DB71 removal.

The optimal dose of acetate (external carbon source) for maximum dye removal are not the unique variable that needs to be controlled for an efficient process. Another strategy called ratio control; keeping the carbon:dye (Acetate/dye) ratio at a certain level by dosing external carbon for the efficient removal of pollutants. From Fig. 5, it was found that ratio alone did not have a straightforward relation to removal achieved, i.e., same ratio did not show the same dye removal efficiency. Dye concentration in feed solution also has a significant role. However, this study only was focused to determine the setpoint for minimum external carbon source to meet the effluent standard.

3.3.2. Interaction between HRT and acetate to dye ratio on anaerobic bio-digestion of dyes

To evaluate the HRT impact on anaerobic bio-digestion of dyes and find out the interaction between the HRT and acetate to dye ratio on the dye removal process, simulations were conducted at various acetate to dye ratio and HRT. The variation of acetate to dye ratio was done by changing acetate concentration 0–1.2 mgCOD/mL over a fixed 0.40 mgCOD/mL DB71 solution. The HRT was set by changing the feed flow rate from 0.03 mL/h to 1.5 mL/h in the bioreactor active biofilm (0.00262 mL). The steady-state removal reached for each combination is depicted in Fig. 6. As expected, HRT influenced the DB71 removal efficiency. Without adding any acetate in the feed solution (acetate to BD71 ratio 0) the DB71 removal was increased from 6.8% to 74.3% as HRT increases from 0.020 to 0.088 h. Increasing HRT provides more time to the microorganisms to digest dye and other intermediate products, thus enhancing the dye removal.

As suspected, both HRT and acetate to dye ratio altered the dye removal efficiency. However, a small amount of external carbon source (acetate) is desired since it makes the process more economical, also in terms of lower sludge production. The optimization addressed here is to interactive performance between HRT and external carbon source to dye ratio. The study enables the reduction of the use of external carbon sources by increasing HRT without hampering the effluent water quality; however, it should be well balanced with HRT to reduce the investment cost.
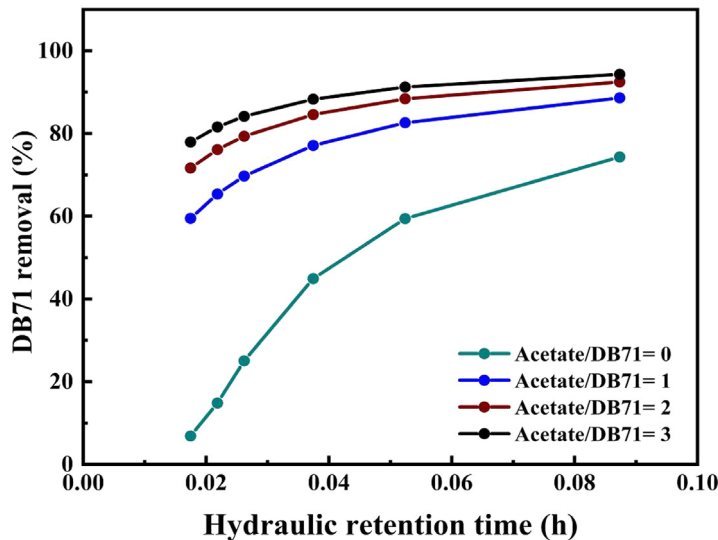
Fig. 6. Effect of HRT and acetate to DB71 ratio on DB71 removal.

4. Conclusions

A mathematical model for anaerobic biodegradation of dyes using biofilm reactors coupled with membrane filtration was developed, calibrated and validated with different types of dye, various feed concentrations and several hydraulic retention times.

Hydrolysis played a major role on the anaerobic biodegradation of dyes becoming the limiting step. The hydrolysis rate constant was dependent on dye molecule structure and biofilm support materials. Increasing molecular weight, as well as the complexity of dye structure, decreased the hydrolysis capacity of dye. Simple dye possesses higher hydrolysis constant compared to more complex (higher molecular weight) dyes.

The support materials, on which the biofilm was formed, have a significant effect on dye removal efficiency. Materials with high electron transfer capacity increases the biofilm activities and hydrolysis as well as enhance the removal efficiency.

External carbon source is also important for efficient dye removal through anaerobic digestion. Increase of the carbon source dose enhances the dye removal efficiency. The required external carbon source for efficient dye removal also depends on the type of dyes; simple dye needs a low external carbon dose compared to more complex dyes. Acetate to dye ratio did not have a straightforward relation to dye removal efficiency since dye feed concentration also needs to be taken into account.

Hydraulic retention time (HRT) enhances the dye removal efficiency. It is possible to compensate lower external carbon source doses with higher HRT to achieve a targeted level of dye removal.

CRediT authorship contribution statement

Mohammad Shaiful Alam Amin: Conceptualization, Methodology, Investigation, Writing – original draft. **Md. Salatul Islam Mozumder:** Methodology, Formal analysis, Software, Writing – original draft. **Frank Stüber:** Resources, Writing – review & editing. **Jaume Giralt:** Software, Writing – review & editing. **Agustí Fortuny:** Validation, Writing – review & editing. **Azael Fabregat:** Validation, Writing – review & editing. **Josep Font:** Funding acquisition, Project administration, Conceptualization, Methodology, Supervision, Writing – review & editing.

Declaration of competing interest

The authors declare that they have no known competing financial interests or personal relationships that could have appeared to influence the work reported in this paper.

Table A.1
Experimental and predicted outcomes of AO7 removal of CSGOM bioreactor.

HRT (h)	$S_{S(in)}$ (mgCOD/mL)	% Deviation
0.040	0.099	7.1
	0.149	8.8
	0.198	8.7
0.027	0.099	8.5
	0.149	6.1
	0.198	7.1
0.020	0.099	9.2
	0.149	6.8
	0.198	8.0

Table A.2
Experimental and predicted outcomes of RB5 removal of CSGOM bioreactor.

HRT (h)	$S_{S(in)}$ (mgCOD/mL)	% Deviation
0.040	0.066	9.0
	0.099	8.2
	0.133	2.8
0.027	0.066	4.8
	0.099	2.7
	0.133	3.0
0.020	0.066	6.5
	0.099	6.8
	0.133	2.1

Table A.3
Experimental and predicted outcomes of DB71 removal of CSGOM bioreactor.

HRT (h)	$S_{S(in)}$ (mgCOD/mL)	% Deviation
0.040	0.089	5.3
	0.134	5.0
	0.179	9.5
0.027	0.089	1.4
	0.134	8.8
	0.179	8.2
0.020	0.089	7.2
	0.134	8.1
	0.179	2.8

Data availability

Data will be made available on request.

Acknowledgments

Appendix

See Tables A.1–A.4.

Table A.4
Experimental and predicted outcomes of DB71 removal of CSCM bioreactor.

HRT (h)	$S_{S(in)}$ (mgCOD/mL)	% Deviation
0.040	0.089	9.0
	0.134	6.9
	0.179	4.1
0.027	0.089	0.02
	0.134	1.6
	0.179	9.6
0.020	0.089	4.3
	0.134	8.9
	0.179	1.8

References

Amin, M.S.A., Stüber, F., Giralt, J., Fortuny, A., Fabregat, A., Font, J., 2021. Comparative anaerobic decolorization of azo dyes by carbon-based membrane bioreactor. Water 13 (8), 1060.

Amin, M.S.A., Stüber, F., Giralt, J., Fortuny, A., Fabregat, A., Font, J., 2022a. Ceramic-supported graphene oxide membrane bioreactor for the anaerobic decolorization of azo dyes. J. Water Process Eng. 45, 102499.

Amin, M.S.A., Stüber, F., Giralt, J., Fortuny, A., Fabregat, A., Font, J., 2022b. Compact carbon-based membrane reactors for the intensified anaerobic decolorization of dye effluents. Membranes 12 (2), 174.

Benkhaya, S., M'Rabet, S., El Harfi, A., 2020. Classifications, properties, recent synthesis and applications of azo dyes. Heliyon 6 (1), e03271.

Berradi, M., Hsissou, R., Khudhair, M., Assouag, M., Cherkaoui, O., El Bachiri, A., El Harfi, A., 2019. Textile finishing dyes and their impact on aquatic environs. Heliyon 5 (11), e02711.

Bibi, A., Zhu, H.-x., Mahmood, Q., Wang, J., Li, X.-D., Mujaddad ur, R., Hayat, T., Shaheen, N., Ali, A., 2020. Efficient bacterial isolate from roots of cactus degrading reactive black 5. Environ. Technol. Innov. 20, 101082.

Cui, M.H., Cui, D., Gao, L., Cheng, H.Y., Wang, A.J., 2016b. Efficient azo dye decolorization in a continuous stirred tank reactor (CSTR) with built-in bioelectrochemical system. Bioresour. Technol. 218, 1307–1311.

Cui, M.-H., Cui, D., Gao, L., Wang, A.-J., Cheng, H.-Y., 2016a. Azo dye decolorization in an up-flow bioelectrochemical reactor with domestic wastewater as a cost-effective yet highly efficient electron donor source. Water Res. 105, 520–526.

Culbertson, J.B., 1951. Factors affecting the rate of hydrolysis of ketimines. J. Am. Chem. Soc. 73 (10), 4818–4823.

da Silva, M.E.R., Firmino, P.I.M., de Sousa, M.R., dos Santos, A.B., 2012. Sequential anaerobic/aerobic treatment of dye-containing wastewaters: Colour and COD removals, and ecotoxicity tests. Appl. Biochem. Biotechnol. 166 (4), 1057–1069.

Fenu, A., Guglielmi, G., Jimenez, J., Spèrandio, M., Saroj, D., Lesjean, B., Brepols, C., Thoeye, C., Nopens, I., 2010. Activated sludge model (ASM) based modelling of membrane bioreactor (MBR) processes: A critical review with special regard to MBR specificities. Water Res. 44 (15), 4272–4294.

García-Martínez, Y., Bengoa, C., Stüber, F., Fortuny, A., Font, J., Fabregat, A., 2015. Biodegradation of acid orange 7 in an anaerobic–aerobic sequential treatment system. Chem. Eng. Process. - Process Intensif. 94, 99–104.

Georgiou, D., Metallinou, C., Aivasidis, A., Voudrias, E., Gimouhopoulos, K., 2004. Decolorization of azo-reactive dyes and cotton-textile wastewater using anaerobic digestion and acetate-consuming bacteria. Biochem. Eng. J. 19 (1), 75–79.

Giménez-Pérez, A., Bikkarolla, S.K., Benson, J., Bengoa, C., Stüber, F., Fortuny, A., Fabregat, A., Font, J., Papakonstantinou, P., 2016. Synthesis of N-doped and non-doped partially oxidised graphene membranes supported over ceramic materials. J. Mater. Sci. 51 (18), 8346–8360.

Hammad, M., Fortugno, P., Hardt, S., Kim, C., Salamon, S., Schmidt, T.C., Wende, H., Schulz, C., Wiggers, H., 2021. Large-scale synthesis of iron oxide/graphene hybrid materials as highly efficient photo-fenton catalyst for water remediation. Environ. Technol. Innov. 21, 101239.

Han, F., Kambala, V.S.R., Dharmarajan, R., Liu, Y., Naidu, R., 2018. Photocatalytic degradation of azo dye acid orange 7 using different light sources over Fe^{3+}-doped TiO_2 nanocatalysts. Environ. Technol. Innov. 12, 27–42.

Hao, X.D., van Loosdrecht, M.C.M., 2004. Model-based evaluation of COD influence on a partial nitrification-anammox biofilm (CANON) process. Water Sci. Technol. 49 (11–12), 83–90.

Henze, M., Gujer, W., Mino, T., van Loosdrecht, M.C.M., 2000. Activated Sludge Models ASM1, ASM2, ASM2d and ASM3. IWA Publishing, London.

Iqbal, A., Ali, N., Shang, Z.-H., Malik, N.H., Rehman, M.M.U., Sajjad, W., Rehman, M.L.U., Khan, S., 2022. Decolorization and toxicity evaluation of simulated textile effluent via natural microbial consortia in attached growth reactors. Environ. Technol. Innov. 26, 102284.

Jankowska, K., Grzywaczyk, A., Piasecki, A., Kijeńska-Gawrońska, E., Nguyen, L.N., Zdarta, J., Nghiem, L.D., Pinelo, M., Jesionowski, T., 2021. Electrospun biosystems made of nylon 6 and laccase and its application in dyes removal. Environ. Technol. Innov. 21, 101332.

Kura, G., 1987. Hydrolysis reaction of inorganic cyclophosphates at various acid strengths. Polyhedron 6 (3), 531–533.

Li, Q., Tang, X., Sun, Y., Wang, Y., Long, Y., Jiang, J., Xu, H., 2015. Removal of rhodamine b from wastewater by modified volvariella volvacea: batch and column study. RSC Adv. 5 (32), 25337–25347.

Mezohegyi, G., Kolodkin, A., Castro, U.I., Bengoa, C., Stuber, F., Font, J., Fabregat, A., Fortuny, A., 2007. Effective anaerobic decolorization of azo dye acid orange 7 in continuous upflow packed-bed reactor using biological activated carbon system. Ind. Eng. Chem. Res. 46 (21), 6788–6792.

Mozumder, M.S.I., Picioreanu, C., van Loosdrecht, M.C.M., Volcke, E.I.P., 2014. Effect of heterotrophic growth on autotrophic nitrogen removal in a granular sludge reactor. Environ. Technol. 35 (8), 1027–1037.

Nguyen, T.H., Watari, T., Hatamoto, M., Sutani, D., Setiadi, T., Yamaguchi, T., 2020. Evaluation of a combined anaerobic baffled reactor–downflow hanging sponge biosystem for treatment of synthetic dyeing wastewater. Environ. Technol. Innov. 19, 100913.

Oh, Y.-K., Kim, Y.-J., Ahn, Y., Song, S.-K., Park, S., 2004. Color removal of real textile wastewater by sequential anaerobic and aerobic reactors. Biotechnol. Bioprocess Eng. 9 (5), 419.

Orhon, D., Yucel, A.B., Insel, G., Duba, S., Olmez-Hanci, T., Solmaz, B., Sözen, S., 2021a. A new activated sludge model with membrane separation-implications for sewage and textile effluent. Membranes (Basel) 11 (8).

Orhon, D., Yucel, A.B., Insel, G., Solmaz, B., Mermutlu, R., Sözen, S., 2021b. Appraisal of super-fast membrane bioreactors by MASM—A new activated sludge model for membrane filtration. Water.

Pandey, A., Singh, P., Iyengar, L., 2007. Bacterial decolorization and degradation of azo dyes. Int. Biodeterior. Biodegrad. 59 (2), 73–84.

Petersen, B., Gernaey, K., Henze, M., Vanrolleghem, P., 2002. Evaluation of an ASM 1 model calibration procedure on a municipal-industrial wastewater treatment plant. J. Hydroinform. 4.

Picioreanu, C., van Loosdrecht, M.C.M., Heijnen, J.J., 1997. Modelling the effect of oxygen concentration on nitrite accumulation in a biofilm airlift suspension reactor. Water Sci. Technol. 36 (1), 147–156.

Reichert, P., 1994. Aquasim – a tool for simulation and data analysis of aquatic systems. Water Sci. Technol. 30 (2), 21–30.

Solís, M., Solís, A., Pérez, H.I., Manjarrez, N., Flores, M., 2012. Microbial decolouration of azo dyes: A review. Process Biochem. 47 (12), 1723–1748.

Sonwani, R.K., Swain, G., Giri, B.S., Singh, R.S., Rai, B.N., 2020. Biodegradation of congo red dye in a moving bed biofilm reactor: Performance evaluation and kinetic modeling. Bioresour. Technol. 302, 122811.

Stewart Philip, S., 2003. Diffusion in biofilms. J. Bacteriol. 185 (5), 1485–1491.

Sun, J., Dai, X., Wang, Q., Pan, Y., Ni, B.-J., 2016. Modelling methane production and sulfate reduction in anaerobic granular sludge reactor with ethanol as electron donor. Sci. Rep. 6 (1), 35312.

Takkar, S., Tyagi, B., Kumar, N., Kumari, T., Iqbal, K., Varma, A., Thakur, I.S., Mishra, A., 2022. Biodegradation of methyl red dye by a novel actinobacterium zhihengliuella sp. ISTPL4: Kinetic studies, isotherm and biodegradation pathway. Environ. Technol. Innov. 26, 102348.

Thung, W.-E., Ong, S.-A., Ho, L.-N., Wong, Y., Ridwan, F., Lehl, H., Oon, Y.-L., Oon, Y.-S., 2017. Biodegradation of acid orange 7 in a combined anaerobic-aerobic up-flow membrane-less microbial fuel cell: Mechanism of biodegradation and electron transfer. Chem. Eng. J. 336.

Tombari, E., Salvetti, G., Ferrari, C., Johari, G.P., 2007. Kinetics and thermodynamics of sucrose hydrolysis from real-time enthalpy and heat capacity measurements. J. Phys. Chem. B 111 (3), 496–501.

Uddin, M.J., Islam, M.A., Haque, S.A., Hasan, S., Amin, M.S.A., Rahman, M.M., 2012. Preparation of nanostructured TiO_2-based photocatalyst by controlling the calcining temperature and pH. Int. Nano Lett. 2 (1), 1–10.

van Benthum, W.A.J., van Loosdrecht, M.C.M., Tijhuis, L., Heijnen, J.J., 1995. Solids retention time in heterotrophic and nitrifying biofilms in a biofilm airlift suspension reactor. Water Sci. Technol. 32 (8), 53–60.

Van Loosdrecht, M.C.M., Henze, M., 1999. Maintenance, endogeneous respiration, lysis, decay and predation. Water Sci. Technol. 39 (1), 107–117.

Volcke, E.I., Picioreanu, C., De Baets, B., van Loosdrecht, M.C., 2010. Effect of granule size on autotrophic nitrogen removal in a granular sludge reactor. Environ. Technol. 31 (11), 1271–1280.

Vu, M.T., Vu, H.P., Nguyen, L.N., Semblante, G.U., Johir, M.A.H., Nghiem, L.D., 2020. A hybrid anaerobic and microalgal membrane reactor for energy and microalgal biomass production from wastewater. Environ. Technol. Innov. 19, 100834.

Williamson, K., McCarty, P.L., 1976. A model of substrate utilization by bacterial films. J. - Water Pollut. Control Fed. 48 (1), 9–24.

Yilmaz Ozmen, E., Erdemir, S., Yilmaz, M., Bahadir, M., 2007. Removal of carcinogenic direct azo dyes from aqueous solutions using calix[n]arene derivatives. Clean – Soil Air Water 35 (6), 612–616.

Yoo, E., Libra, J., Adrian, L., 2001. Mechanism of dye reduction of azo dyes in anaerobic mixed culture. J. Environ. Eng.-Asce - J. Environ. Eng.-ASCE 127.